Morphology and Electrical Properties of Polymethylmethacrylate/Poly(styrene-*co*-acrylonitrile)/ Multi-Walled Carbon Nanotube Nanocomposites

Minho Lee, Hyeonyeol Jeon, Byong Hun Min, Jeong Ho Kim

Department of Chemical Engineering, University of Suwon, Gyeonggi-do 445-743, Korea

Received 10 May 2010; accepted 23 November 2010
DOI 10.1002/app.33819
Published online 23 February 2011 in Wiley Online Library (wileyonlinelibrary.com).

ABSTRACT: Nanocomposites of blends of polymethylmethacrylate (PMMA) and poly(styrene-*co*-acrylonitrile) (SAN) with multi-walled carbon nanotubes (MWCNTs) were prepared by melt mixing in a twin-screw extruder. The dispersion state of MWCNTs in the matrix polymers was investigated using transmission electron microscopy. Interestingly enough, in most of the nanocomposites, the MWCNTs were observed to be mainly located at SAN domains, regardless of the SAN compositions in the PMMA/SAN blend and of the processing method. One possible reason for this morphology may be the π–π interactions between MWCNTs and the phenyl ring of SAN. The shift in G-band peak observed in the Raman spectroscopy may be the indirect evidence proving these interactions. The percolation threshold for electrical conductivity of PMMA/SAN/MWCNT nanocomposites was observed to be around 1.5 wt %. Nanocomposites with PMMA-rich composition showed higher electrical conductivity than SAN-rich nanocomposites at a fixed MWCNT loading. The dielectric constant measurement also showed composition-dependent behavior. © 2011 Wiley Periodicals, Inc. J Appl Polym Sci 121: 743–749, 2011

Key words: nanocomposite; multi-walled carbon nanotube; morphology

INTRODUCTION

Multi-walled carbon nanotubes (MWCNTs) have extraordinary mechanical, electrical, thermal, and optical properties that make them highly interesting for applications in materials science.[1–3] In recent years, polymer/MWCNT nanocomposites have been extensively studied, especially in regards to the interfacial phenomena between MWCNTs and polymers in achieving various excellent properties of nanocomposites as compared to conventional composites. In the nanocomposites of a polymer with MWCNTs, the interaction behavior between matrix polymers and MWCNTs has a great effect on the dispersion state of MWCNT within nanocomposites. The nanocomposites of polymer blends with MWCNTs become complicated and even interesting since in some cases percolation threshold values of polymer blend nanocomposites can be lowered further than those of nanocomposites of a single polymer with the MWCNT.

Although polymer/MWCNT nanocomposites have been widely studied using different preparation methods, such as *in situ* polymerization, solution blending and melt mixing, not much literature is dedicated to studying the nanocomposites of polymer blends with MWCNTs.

It is well known that the mixture of polymethylmethacrylate (PMMA) and poly(styrene-*co*-acrylonitrile) (SAN) mixed together forms a miscible blend. It has been suggested that the origin of PMMA/SAN blend miscibility results from the repulsion effect between styrene and acrylonitrile units in SAN. This indicates that the miscibility of the blend is not very strong compared to blends involving specific interactions between the blend components.[4,5] PMMA is reported to be miscible with SAN depending on whether the AN composition in SAN is in the range of between 9.4 and 34.4 wt %.[6–12] PMMA/SAN blends show lower critical solution temperature (LCST) behavior. The cloud point for 50/50 blends is reported to be around 180°C,[13] which is below the usual melt processing temperature of PMMA or SAN. Usual processing temperature, 230°C, is above the phase separation temperature of the PMMA/SAN blend. Therefore, phase separation occurs during melt processing when PMMA and SAN are melt mixed with MWCNT in the extruder. It can be assumed that the variations in domain shape and size formed by phase separation behavior have an influence on various properties in PMMA/SAN/MWCNT nanocomposites.

Previous studies modify MWCNTs with maleic anhydride for better dispersion of MWCNT. Nanocomposites of this maleic-anhydride-grafted-

Correspondence to: J. H. Kim (jhkim@suwon.ac.kr).

MWCNT and PMMA were prepared via in-polymerization.[14,15] Related literature also mentions grafting of SAN onto MWCNTs.[16–21] It is also known that PMMA-grafted MWCNTs can be effectively dispersed in the SAN matrix.[22]

In this study, nanocomposites of PMMA/SAN blend with MWCNT were prepared by melt processing in the twin-screw extruder and the morphology and physical properties of nanocomposites were investigated. Electrical conductivity analysis, transmission electron microscopy (TEM), dielectric analysis, and Raman spectroscopy were conducted to investigate MWCNT dispersion and its influence on the physical properties of nanocomposites.

EXPERIMENTAL

Materials

The polymers used in this study were PMMA (LG Chem., Melt Index: 5.8) and SAN (AN content: 26 wt %, LG Chem., Melt Index: 10). MWCNTs (CM-95) with about 95 wt % purity were obtained from Hanwha Nanotech Corp. The diameter, length and surface area of MWCNTs were 10–15 nm, 10–20 μm, and 200 $m^2\ g^{-1}$, respectively. MWCNTs were used as obtained without further purification.

Preparation of PMMA/SAN/MWCNT nanocomposites

Prior to use, the MWCNTs were dried for 24 h in a vacuum oven to remove all moisture. PMMA and SAN were also dried for 4 h at 80°C before all components were blended in the extruder. The MWCNT loadings of all nanocomposite samples were set at 1, 1.5, 2, and 3 wt %. PMMA, SAN and MWCNTs were fed into the extruder at the same time and melt mixed in the twin-screw extruder (Bautek corp. BA-19ST). The nanocomposites were processed at temperatures varying from 200 to 230°C, depending on their position in the extruder. The extrudates from the extruder were pelletized, and then pressed in the hot press into test specimens. Nanocomposites were also prepared using a two-step processing method to procure specimens utilizing an alternative processing method. In the two-step mixing process, one of the polymers to be blended was melt mixed with MWCNTs in the first step and the extrudate from this first step was melt mixed again with the other polymer in the next step.

Characterization and measurements

TEM images of nanocomposite specimens were obtained at the Korea Basic Science Institute using Energy Filtering Transmission Electron Microscopy (EM-912 OMEGA, Carl Zeiss) with an operating voltage of 120 kV. TEM specimens were prepared by encapsulating nanocomposites in epoxy resin and microtoming at room temperature.

Raman spectroscopy (T64000, HORIABA jobin Yvon, France) was done using 514 nm Ar laser and 80 mW laser power to investigate the interactions between MWCNT and polymer in the nanocomposites. The resolution and wavelength range of the lasers were 0.6 cm^{-1} and 0–3500 cm^{-1}, respectively. Dielectric analysis (Precision Impedance Analyzer, Agilent 4294A, Hewlett–Packard) was conducted at 25°C and from 40 Hz to 300 kHz at 100 mV. Electrical volume resistivity was measured using a multi-meter (Protek 608) at 2.5 V and a high-resistance meter (SM-8210, TOA electronic) with two-point probe at 50 V.

RESULTS AND DISCUSSION

Morphology of PMMA/SAN/MWCNT nanocomposites

TEM images of a PMMA/MWCNT nanocomposite and a SAN/MWCNT nanocomposite each containing 3 wt % MWCNT are shown in Figure 1(a,b), respectively. In Figure 1(a), MWCNTs exhibit fairly good dispersion, with some aggregates of MWCNTs in some areas. In Figure 1(b), MWCNTs demonstrate very good dispersion in its SAN matrix. Comparing Figure 1(a,b), MWCNTs in a SAN matrix show better dispersion than those in PMMA, although the difference between the two is quite small.

Figure 2 shows the TEM images of PMMA/SAN/MWCNT nanocomposites containing 1.5 wt % MWCNT where PMMA, SAN, and MWCNTs were all fed and melt mixed together at the same time in the twin screw extruder. The ratio of PMMA and SAN was changed to be 9/1, 5/5, and 1/9, the TEM pictures for which are shown in Figure 2(a–c), respectively. The phase-separated morphologies are clearly visible in these pictures of PMMA/SAN/MWCNT nanocomposites. This is quite natural since the PMMA/SAN forms a miscible blend at room temperature and begins to phase-separate at temperature above 180°C. In this study, PMMA and SAN were melt-blended in the twin-screw extruder at 230°C. Upon melting in the extruder, they may have formed a miscible blend at the beginning followed by immediate phase-separation due to the high processing temperature. In Figure 2, the bright area is PMMA, and the dark one represents SAN.

In the nanocomposites of PMMA/SAN(9/1) containing 1.5 wt % MWCNT (referred to as P/S(9/1)-1.5 hereinafter) shown in Figure 2(a), SAN is observed to form the dispersed phase. This is expected considering PMMA's rich composition. Nanocomposites of P/S(1/9)-1.5 with SAN-rich

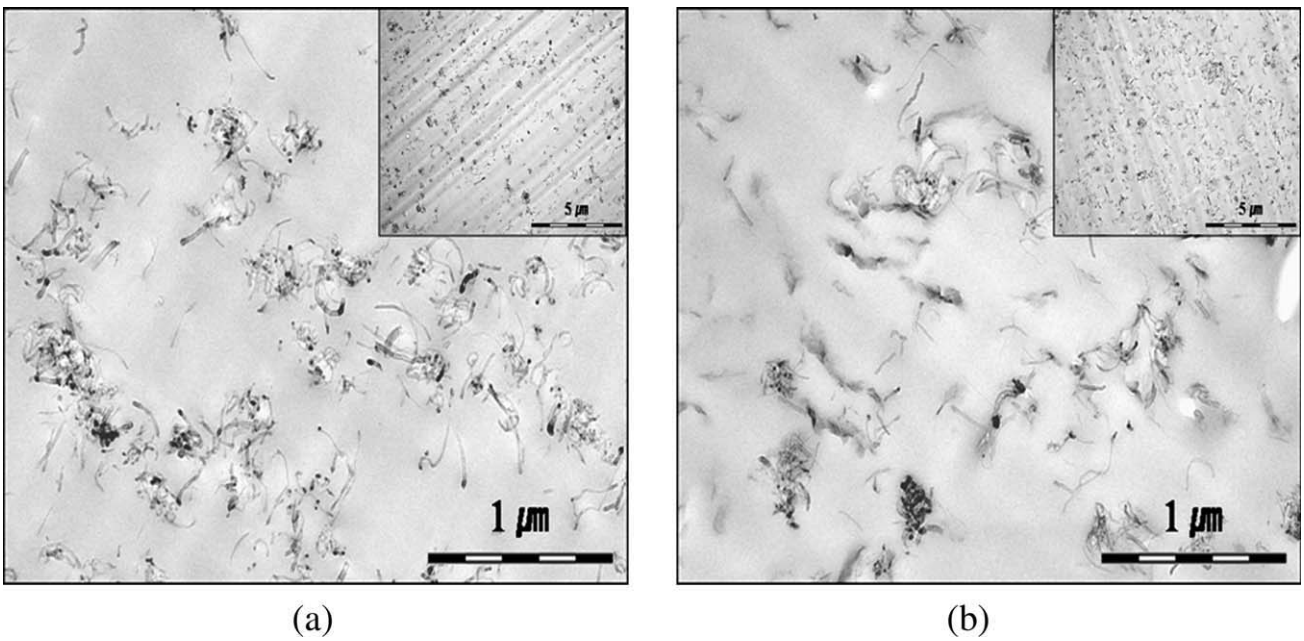

Figure 1 TEM images of nanocomposites of (a) PMMA/MWCNT and (b) SAN/MWCNT containing 3 wt % MWCNT. Insets are lower magnification images.

composition as seen in Figure 2(c) show the PMMA-dispersed phase. P/S(5/5)-1.5 in Figure 2(b) shows the cocontinuous phase as also expected. One thing remarkable in these pictures is that most of MWCNTs are observed to be located in the SAN phase regardless of the SAN composition and whether SAN forms a dispersed phase or continuous phase. Specifically, when SAN is the dispersed phase at the ratio of 9/1(PMMA/SAN), most of the MWCNTs are located in those small SAN-dispersed domains.

To check if other morphology can be achieved by changing the processing method, nanocomposites of PMMA/SAN(5/5) containing 1.5 wt % MWCNT (P/S(5/5)-1.5) were prepared by changing the melt mixing method into two-step mixing. Two types of two-step mixing experiments were conducted. In one experiment, MWCNTs were mixed with PMMA first, then the resulting extrudate was again mixed with SAN. TEM pictures of the samples prepared by this method ((PMMA-MWCNT)/SAN) are presented in Figure 3(a).

In the second experiment, the sequence was reversed, with MWCNTs mixed with SAN first, then the resulting extrudate mixed with PMMA. The morphology of the samples prepared according to the second procedure ((SAN-MWCNT)/PMMA) can be seen in Figure 3(b). Interestingly enough, similar morphology to that shown in Figure 2(b) was obtained for both samples as shown in Figure 3(a,b), which are prepared by different processing sequences with the same composition. Most of MWCNTs are observed to be mainly located in the SAN phase despite different processing sequences. It is worth noting that the MWCNTs that were mixed with PMMA first and located in PMMA moved to the SAN phase during the mixing of extrudates with SAN since MWCNTs were observed to be in the SAN phase in the final nanocomposites.

Results of the above experiment indicate that the location of MWCNTs in the SAN phase is not determined by processing method but by the thermodynamic affinity between polymers and MWCNTs, since different processing sequences still produced the same morphology. It also indicates that SAN has higher affinity with MWCNTs than PMMA. This may be due to the phenyl ring of SAN, which may interact with the graphene sheet of MWCNT. One instance of this may be an interaction between aromatic moieties and MWCNTs reported in the literature.[23] A similar type of interaction was also considered relevant to polyethylene terephthalate (PET)/MWCNT nanocomposites.[24] Since π–π interactions are caused by the intermolecular overlapping of *p*-orbitals in π-conjugated systems, it is expected that the phenyl-ring structure interacts strongly with the graphene sheet of the nanotube surface through the intermolecular overlap of π-orbitals (π-stacking). To see if there exists any interaction between SAN and MWCNTs, Raman spectroscopy was applied to this nanocomposite system.

Raman spectroscopy results

Figure 4 shows the Raman spectra of neat MWCNT and PMMA/SAN nanocomposites containing 1.5 wt %

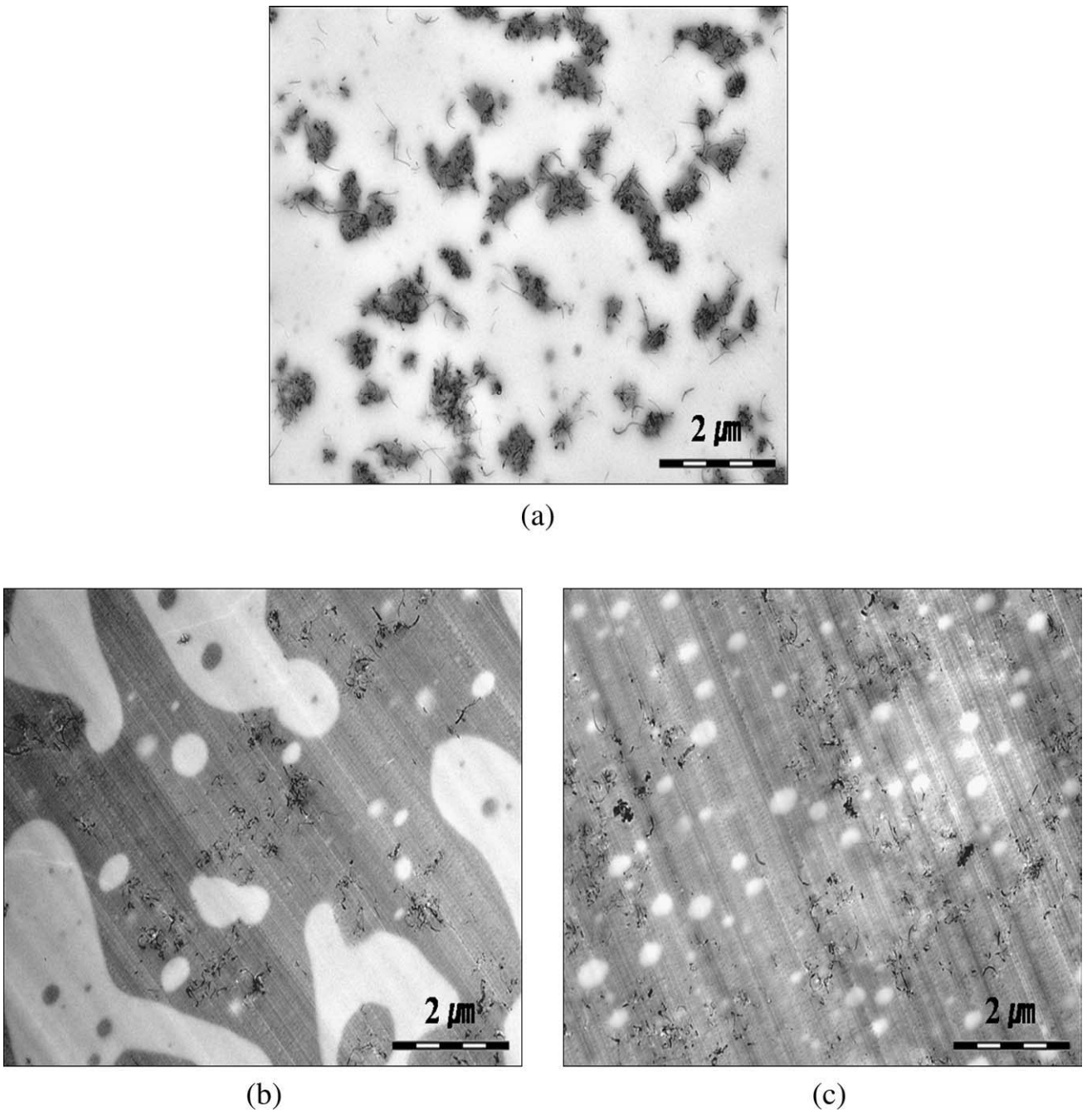

Figure 2 TEM images of PMMA/SAN/MWCNT nanocomposites containing 1.5 wt % MWCNT: (a) PMMA/SAN(9/1), (b) PMMA/SAN(5/5), and (c) PMMA/SAN(1/9).

MWCNT. Peaks around 1350 and 1590 cm^{-1} are referred to as D and G band, respectively; G band is known to originate from MWCNT.[25] In this spectra, the positions of this G band for P/S(1/9)-1.5, P/S(5/5)-1.5, and P/S(1/9)-1.5 are 1584, 1592, and 1596, respectively, while that of neat MWCNT is 1584. This means that the shift in this peak is observed for P/S(5/5)-1.5 and P/S(1/9)-1.5 compared to neat MWCNT. It is noted that the amount of shift increases in accordance with increasing SAN contents in SAN-rich nanocomposites. This indicates that there may exist an interaction between SAN and MWCNT. P/S(9/1)-1.5 being rich in PMMA composition did not show the noticeable shift depicted in Figure 4.

The number of interaction sites between MWCNT and SAN in this nanocomposite may be too small to show a shift in the Raman spectra since the amount of SAN in this nanocomposite may be insufficient to produce noticeable change. Again, the interaction may be between the phenyl group in the styrene portion of SAN and the graphene sheets of MWCNT surface. Along with the observation based on TEM

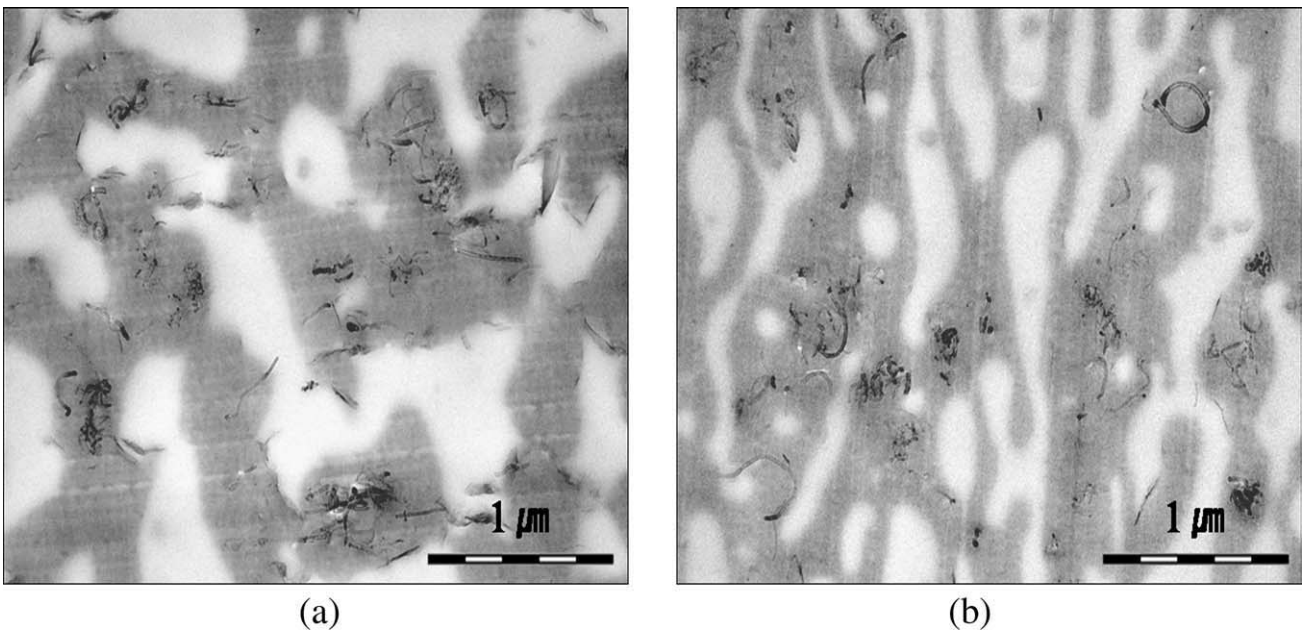

Figure 3 TEM images of PMMA/SAN/MWCNT nanocomposites containing 1.5 wt % MWCNT prepared by (a) mixing of PMMA and MWCNT first followed by mixing with SAN and (b) mixing of SAN and MWCNT first followed by mixing with PMMA.

pictures that MWCNTs are mainly located at SAN domains, this shift in Raman spectra could be another indication of interaction between SAN and MWCNTs.

Electrical conductivity and dielectric properties of PMMA/SAN/MWCNT nanocomposites

Figure 5 shows the results of electrical volume resistivity of PMMA/SAN/MWCNT nanocomposites prepared by simultaneous mixing of three components. This result exhibits that the electrical percolation threshold value of PMMA/SAN/MWCNT hovers around 1.5 wt %.

It is noted that the electrical resistivity varies depending on the SAN composition at a fixed MWCNT loading. Especially at 1.5 wt % MWCNT loading, the electrical resistivity values of SAN-rich compositions were observed to be higher than those of PMMA-rich compositions. This means that the electrical conductivity of SAN-rich compositions is

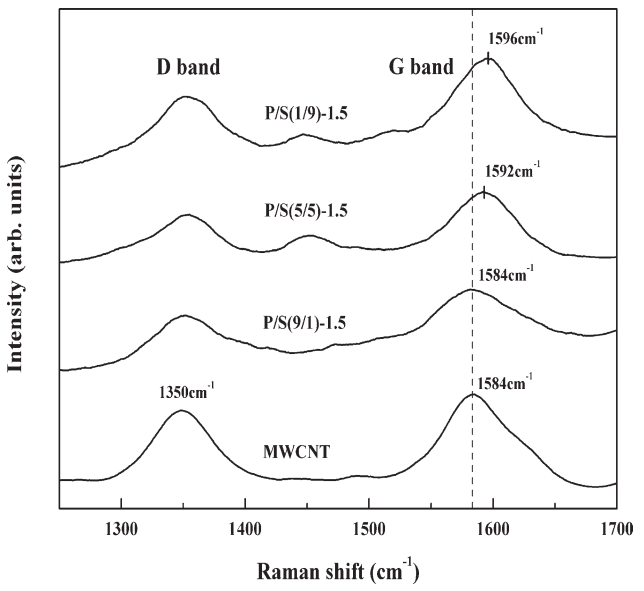

Figure 4 Raman spectra of PMMA/SAN/MWCNT nanocomposites.

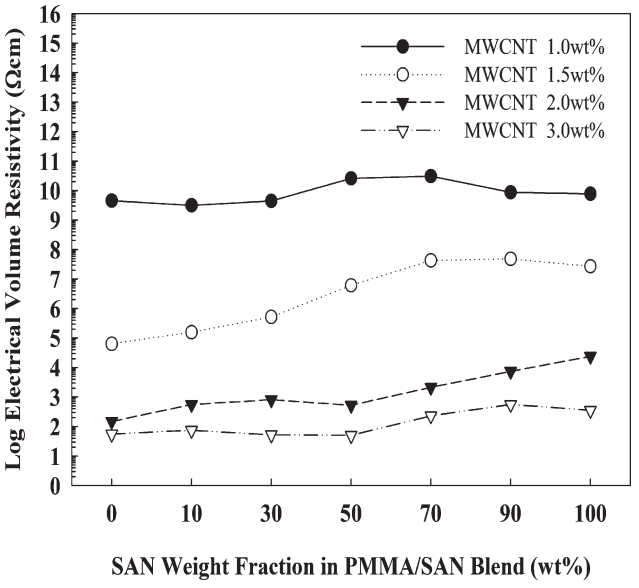

Figure 5 Electrical volume resistivity of PMMA and SAN blend as a function of SAN composition at various MWCNT loadings.

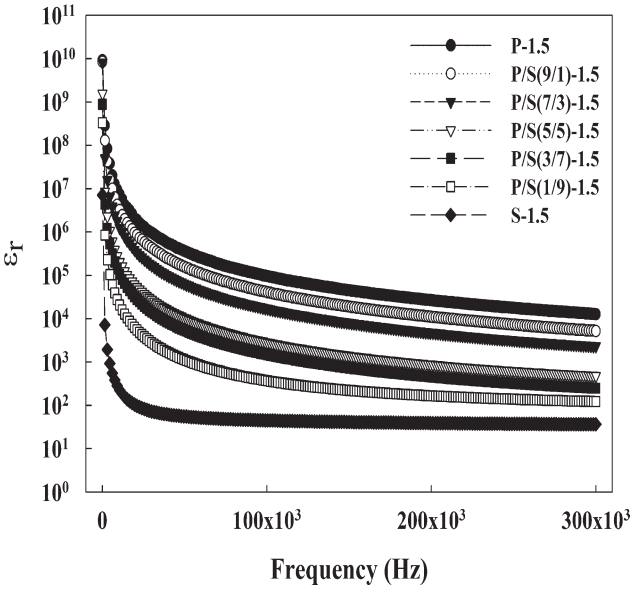

Figure 6 Dielectric constants as a function of frequency at various compositions of PMMA and SAN.

lower than that of PMMA-rich compositions. This result is somewhat unexpected, since in the morphology analysis, most of the MWCNTs were located in the SAN-continuous phase of SAN-rich compositions such as with the ratio of 1/9(PMMA/SAN) as indicated in Figure 2(c). This kind of morphology usually indicates high conductivity, since MWCNTs may relatively easily form network structure in the continuous phase. Also, when SAN in PMMA-rich compositions is in dispersed phase, such as with the ratio of 9/1(PMMA/SAN), most of the MWCNTs are located in small, SAN-dispersed domains [Fig. 2(a)], in which case low electrical conductivity is expected. But again, the experiment resulted in higher conductivity in the PMMA-rich compositions rather than the SAN-rich compositions.

To study the cause behind this, the dielectric constants were also measured for these nanocomposites. It was reported in the literature that electrical conductivity could be directly related to the dielectric constant such that both the dielectric constant and electrical conductivity increase concurrently with increasing MWCNT composition in polymer/MWCNT nanocomposites.[26]

Figure 6 shows the variation of relative dielectric constants (ε_r) of PMMA/SAN/MWCNT nanocomposites containing 1.5 wt % MWCNT with frequency changes depending on the composition of PMMA and SAN at room temperature. The dielectric constant of PMMA with 1.5 wt % MWCNT shows the highest value. As the composition of SAN increases in PMMA/SAN/MWCNT, the dielectric constant progressively decreases until the lowest value is reached for SAN/MWCNT. This result is consistent with the electrical resistivity result shown in Figure 6, since in the literature a high dielectric constant is known to produce high electrical conductivity.[26]

From the results of electrical conductivity and dielectric constant measurement, PMMA is observed to become more conductive by adding MWCNTs rather than SAN. This is particular true of PMMA/SAN(9/1)-1.5 containing 1.5 wt % MWCNT, which become more conductive than PMMA/SAN(1/9)-1.5 even though MWCNTs are mainly located in a SAN-dispersed phase. As shown in Figure 2(a) for PMMA/SAN(9/1)-1.5, SAN domains containing MWCNTs may form loose network structures although those SAN-dispersed domains are not completely connected due to the interruption by PMMA-continuous phase. Although the SAN domains are not completely connected, electrons are thought to jump from one SAN domain to another through PMMA relatively easily, since PMMA has relatively good conductivity compared to SAN.

Figure 7 shows the TEM image of 9/1(PMMA/SAN) nanocomposites containing 1.5 wt % MWCNT, a higher magnification image than that shown in Figure 2(a). Although most of MWCNTs are seen to be located in the SAN domains, small fractions of MWCNTs are observed in the PMMA phase. These MWCNTs outside the SAN domains may help forming the conductive paths contributing a little bit for the higher electrical conductivity. In PMMA/SAN(1/9)-1.5 showing lower conductivity than PMMA/SAN(9/1)-1.5, good dispersion of MWCNTs can be seen such as in Figure 2(c), where MWCNTs are dispersed in the SAN-continuous phase. But in this case, MWCNTs are not completely connected,

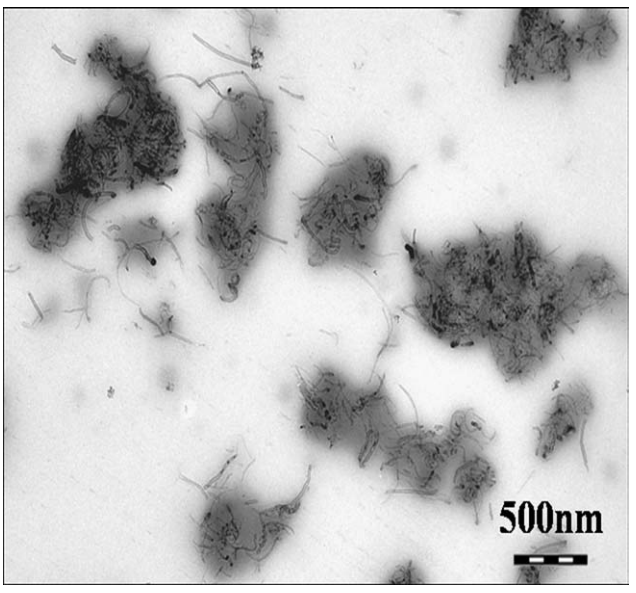

Figure 7 High magnification TEM image of PMMA/SAN(9/1) nanocomposites containing 1.5 wt % MWCNT (500 nm scale).

and the movement of electrons through SAN regions without MWCNT may not be as easy as movement through PMMA. This may result in the relatively low conductivity of PMMA/SAN(1/9)-1.5 even though MWCNTs are mainly located in SAN-continuous phase.

Higher polarity of PMMA than SAN is thought to be one of the reasons for better conductivity of PMMA with MWCNT though there may be other factors to be considered.[27] In terms of solubility, the polar (δ_p) component of the Hansen solubility parameter for PMMA is 10.5 while that of SAN is 7.4.[28] This means that PMMA has relatively higher polarity than SAN.

CONCLUSIONS

MWCNTs were shown to be mainly located at SAN phase in nanocomposites with blends of PMMA and SAN. This result may be due to interactions from π–π stacking of phenyl groups in SAN and graphene sheets of MWCNT. Shifts in G-band of Raman spectra were shown to be another indication of this interaction. The percolation threshold of electrical volume resistivity was observed to be around 1.5 wt %. With the increase in PMMA content in nanocomposites containing 1.5 wt % MWCNT, electrical conductivity also increases regardless of whether PMMA is in continuous phase or not. Polarity of the polymer was considered to be one of the factors contributing to this behavior. Dielectric constant measurement also indicated composition-dependent behavior.

The authors thank the Korea Basic Science Institute for their provision of high-quality TEM pictures.

References

1. Gorga, R. E.; Cohen, R. E. J Polym Sci B Polym Phys 2004, 42, 2690.
2. Zhao, P.; Wang, K.; Yang, H.; Zhang, Q.; Du, R. N.; Fu, Q. Polymer 2007, 48, 5688.
3. Dondero, W. E.; Gorga, R. E. J Polym Sci B Polym Phys 2006, 44, 864.
4. Kambour, R. P.; Bendler, J. T.; Bopp, R. C. Macromolecules 1983, 16, 753.
5. Paul, D. R.; Barlow, J. W. Polymer 1984, 25, 487.
6. Suess, M.; Kressler, J.; Kammer, H. W. Polymer 1987, 28, 957.
7. Nishimoto, M.; Keskkula, H.; Paul, D. R. Polymer 1989, 30, 1279.
8. Cowie, J. M. G.; Reid, V. M. C.; McEwen, I. J. Polymer 1990, 31, 486.
9. Fowler, M. E.; Keskkula, H.; Paul, D. R. Polymer 1987, 28, 1703.
10. Fowler, M. E.; Barlow, J. W.; Paul, D. R. Polymer 1987, 28, 2145.
11. McMaster, L. P. In Copolymers, Polyblends, and Composites, Platzer, N. A. J., Ed., Advanced Chemical Series No 142, American Chemical Society; Washington DC, 1975, Chapter 5.
12. Bernstein, R. E.; Cruz, C. A.; Paul, D. R.; Barlow, J. W. Macromolecules 1977, 10, 681.
13. Du, M.; Gong, J.; Zheng, Q. Polymer 2004, 45, 6725.
14. Huang, Y. L.; Yuen, S. M.; Ma, C. C. M.; Chuang, C. Y.; Yu, K. C.; Teng, C. C. Compos Sci Technol 2009, 69, 1991.
15. Yuen, S. M.; Ma, C. C. M.; Chuang, C. Y.; Yu, K. C.; Wu, S. Y.; Yang, C. C. Compos Sci Technol 2008, 68, 963.
16. Shi, J. H.; Yang, B. X.; Goh, S. H. Eur Polym Mater 2009, 45, 1002.
17. Kim, K. H.; Jo, W. H. Macromolecules 2007, 40, 3708.
18. Lee, J. U.; Huh, J.; Kim, K. H.; Park, C.; Jo, W. H. Carbon 2007, 45, 1051.
19. Wang, M.; Pramoda, K. P.; Goh, S. H. Carbon 2006, 44, 613.
20. Chen, M.; Wei, Z.; Yuefeng, Z.; Lijun, J.; Renping, Z.; Nikhil, K. Carbon 2008, 45, 706.
21. Petrov, P.; Lou, X.; Pagnoulle, C.; Jerome, C.; Calberg, C.; Jerome, R. Macromol Rapid Commun 2004, 25, 987.
22. Wang, M.; Pramoda, K. P.; Goh, S. H. Polymer 2005, 46, 11510.
23. Scalia, G.; Lagerwall, J. P. F.; Haluska, M.; Dettlff-Weglikowska, U.; Giesselmann, F.; Roth, S. Phys Status Solidi B 2006, 243, 3238.
24. Yoo, H. J.; Jung, Y. C.; Cho, J. W. J Polym Sci B Polym Phys 2008, 46, 900.
25. Ishii, S.; Nagao, M.; Watanabe, T.; Tsuda, S.; Yamaguchi, T.; Takano, Y. Phys C 2009, 469, 1002.
26. Tjong, S. C.; Liang, G. D.; Bao, S. P. Script Mater 2007, 57, 461.
27. Serin, M.; Sakar, D.; Cankurtaran, O.; Karaman, F. J Optoelectron Adv Mater 2005, 7, 1533.
28. Barton, A. F. M. CRC Handbook of Polymer-Liquid Interaction Parameters and Solubility Parameters; CRC Press: Boca Raton, Florida, 1990.